




Nickel–cobalt oxide nanosheets asymmetric supercapacitor for energy storage applications

S. Alrousan¹, B. Albiss^{2,*} , B. Aljawrneh³, A. Alshanableh¹, Amani Al-Othman⁴, and H. Megdadi²

¹Department of Physics, Jordan University of Science & Technology, P.O. Box 3030, Irbid 22110, Jordan

²Nanotechnology Institute, Jordan University of Science & Technology, P.O. Box 3030, Irbid 22110, Jordan

³Department of Physics, Al-Zaytoonah University of Jordan, P.O. Box 130, Amman 11733, Jordan

⁴Department of Chemical Engineering, American University of Sharjah, Sharjah 26666, UAE

Received: 30 November 2022

Accepted: 1 February 2023

Published online:
2 March 2023

© The Author(s), under exclusive licence to Springer Science+Business Media, LLC, part of Springer Nature 2023

ABSTRACT

Supercapacitors are a promising candidate in applications that necessitate high electrochemical stability and storage energy. In this study, NiCo₂O₄ nanosheets were prepared hydrothermally on an ITO substrate and investigated to be utilized as supercapacitor electrodes. The morphology of NiCo₂O₄ nanosheets was examined by scanning electron microscopy (SEM) and atomic force microscopy (AFM). The SEM results showed a 3D-flower-like nanostructure with interconnected nanosheets which was confirmed by the AFM results. However, X-ray fluorescence (XRF) results showed that the as-prepared sample has stoichiometry of Nickel (1) : Cobalt (2). The electrochemical measurements of the as-prepared NiCo₂O₄ supercapacitor electrode such as cyclic voltammetry (CV) and galvanostatic charge/discharge (GCD) studies were done in a two-electrode system with 1.0 M KOH and 1.0 M H₂SO₄. CV curves showed quasi-rectangular shape and high electrochemical stability in KOH and H₂SO₄ electrolyte solutions. In addition, the integral areas of CV curves for both electrolytes are almost identical, indicating efficient charge transfer and ion transport at the electrode/electrolyte interface. Electrochemical impedance spectroscopy (EIS) curves of KOH and H₂SO₄ electrolyte revealed a significant difference. This difference indicates that, the charge transfer in H₂SO₄ electrolyte is faster than charge transfer in KOH, resulting in a linear behavior of the EIS curve. A fabricated hybrid asymmetric supercapacitor (SC) composed of NiCo₂O₄/ITO anode and graphite/ITO cathode delivered a specific capacity of around 235 F/g in KOH solution and 723 F/g in H₂SO₄ electrolyte at 10 mV/s scan rate. The superior electrochemical performances could be attributed to the large surface area that facilitates charge transfer at the electrode/electrolyte interface.

Address correspondence to E-mail: bbalbiss@just.edu.jo

1 Introduction

Supercapacitors, batteries, and fuel cells, all use energy storage mechanisms to store energy in an electrochemical form [1–3]. High-performance approaches in these types of power sources, including supercapacitors in particular, have drawn interest from researchers. Supercapacitors, often referred to as electrochemical capacitors or electrode materials, have attracted interest in the field of energy storage due to their exceptional cycle stability, high reliability, rapid charge/discharge rate, and high power density. Supercapacitors are divided into three categories depending on their charge storage mechanism, asymmetric (or hybrid), electrical double layer, and pseudocapacitive capacitors [4].

Supercapacitor electrodes' material such as metal hydroxides, oxides, and conductive polymers primarily influences the electrochemical capacitor performance, as it determines the nature and magnitude of the charge storage processes occurring within the electrode, such as redox reactions (faradaic; pseudocapacitance) and the double-layer capacitance (non-Faradic) [5]. Also, supercapacitor electrodes can be prepared in different techniques show high electrical conductivity and multiple redox active sites resulting in a high electrochemical activity performance [6–8].

Metal hydroxides, oxides, and conductive polymers are the most often studied pseudocapacitive materials [9]. These materials have a variety of oxidation states and/or structural changes that permit a variety of redox processes [10]. For instance, cobalt hydroxide [Co(OH)₂], cobalt oxide (Co₃O₄), nickel oxide (NiO), and nickel hydroxide [Ni(OH)₂] have been investigated as ideal electrode materials owing to their high pseudocapacitance [11–15]. Moreover, binary metal oxides such as NiMnO₃ exhibit a specific capacitance of 750.2 F/g at a scan rate of 1 mV/s [16], NiCo₂O₄ nanorods, and ultrathin nanosheets on carbon (CNF@NiCo₂O₄) exhibit a specific capacitance of 902 F/g at a current density of 2 A/g [17].

Electrolytes are essential for achieving electrochemical stability and boosting energy density. Additionally, it has the potential to improve charge transfer between the cathode and anode. Currently three types of electrolyte have been used in supercapacitors: organic electrolyte, electrolyte, and aqueous liquids. Aqueous electrolytes such as acidic (H₂SO₄ solution) and alkaline (KOH solution)

provide both higher ionic concentration and lower resistance compare to nonaqueous electrolytes [18, 19]. As a result, their high performance was correlated with their higher conductivity, larger dielectric constant, and larger interfacial area, especially for small electrolyte ions [19, 20].

In this work, a supercapacitor device was designed using binary metal oxide (NiCo₂O₄) thin film as a novel electrode material deposited via hydrothermal technique on ITO substrate. The fabricated device morphological and chemical characteristics were analyzed using scanning electron microscope (SEM), atomic force microscope (AFM), and X-ray fluorescence (XRF). Moreover, the electrochemical measurements were investigated in order to quantify the capability of the supercapacitor device for energy storage, in addition to the role of aqueous electrolytes (potassium hydroxide: KOH and sulfuric acid: H₂SO₄) on the performance of the supercapacitor device and charging/discharging process. Finally, the charge storage mechanism of the prepared asymmetric supercapacitor electrodes was analyzed based on charge-transfer mechanism and device engineering.

2 Experimental

2.1 Materials

Nickel nitrate (II) hexahydrate [Ni(NO₃)₂·6H₂O], cobalt nitrate (II) hexahydrate (Co(NO₃)₂·6H₂O), hexamethylenetetramine (HMTA), and potassium hydroxide (KOH) and sulfuric acid (H₂SO₄) solutions were all obtained from Sigma-Aldrich Chemical Co, St. Louis, MO, USA.

2.2 Electrodes' synthesis

NiCo₂O₄ thin films as a supercapacitor electrodes were prepared by the hydrothermal method in the following steps, a 0.1MHMTA solution was added to an aqueous solution of Ni(NO₃)₂·6H₂O and Co(NO₃)₂·6H₂O of molar ratio (0.1 : 0.2), respectively. The solution was kept under stirring for 15 min to obtain a homogenous solution. Then, the ITO substrate was immersed in the solution and heated in an oven at 140 °C for 2 h. After that, the NiCo₂O₄ thin film formed on the ITO substrate was washed with DI water to remove any residues. Finally, the NiCo₂O₄ thin film was annealed for 2 h at 400 °C.

2.3 Structural and electrochemical characterization

The morphological features and chemical composition of NiCo_2O_4 thin film were studied by means of scanning electron microscopy (SEM), atomic force microscopy (AFM), and X-ray fluorescence (XRF). SEM imaging was obtained by (Quanta FEG 450), AFM imaging was obtained by (SPM SmartSPMTM-1000), and XRF analysis was performed using (NEX QC + QuantEZ, Rigaku) at Nanotechnology Institute at Jordan University of Science and Technology.

As shown in Fig. 1, schematic diagram of supercapacitor-based NiCo_2O_4 anode (working electrode) and graphite cathode (a slurry of graphite that was uniformly coated onto a piece of clean ITO substrate) in KOH and H_2SO_4 electrolytes. It is clearly that, the positive charges produced through electrochemical reaction pathway accumulated on the NiCo_2O_4 surface to form pseudocapacitive charge layer. Meanwhile, negative charges accumulated on the surface of graphite electrode to form electric double-layer capacitor.

The electrochemical performances of the as-prepared sample were measured in two-electrode setup, including the as-prepared working electrode, and 1 M KOH and 1 M H_2SO_4 aqueous solution as the electrolyte. AUTOLAB (PGSTAT302N) electrochemical workstation was employed to perform the electrochemical impedance spectroscopy (EIS), cyclic voltammetry (CV), and galvanostatic charge – discharge measurements of NiCo_2O_4 thin-films electrode materials. Cyclic voltammograms were measured at various scan rates (10, 30, 50, and 100

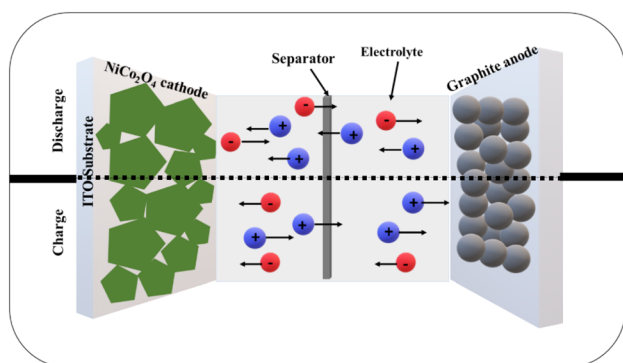


Fig. 1 Schematic diagram illustrates ions diffusion across separator between two electrodes of NiCo_2O_4 anode and graphite cathodes. The effective mass of NiCo_2O_4 and Graphite on top of the ITO substrates are 0.02 mg, and 0.34 g, respectively

mV/s within a potential window ranging from -0.1 to $+0.8$ V. Electrochemical impedance spectroscopy (EIS) was measured by applying an AC voltage of 5 mV amplitude in a frequency range within 0.01 Hz – 100 kHz.

3 Results and discussion

3.1 Surface morphology and structure analysis

The surface morphology and cross-sectional of the as-prepared NiCo_2O_4 sample obtained from SEM images are shown in Fig. 2. The images reflected the 3D-flower-like nanostructure composed of interconnected nanosheets at different scales. The porous structure observed in Fig. 2a, b provides more active sites and promotes the diffusion of electroactive ions and transport of protons in electrolytes, resulting in higher electrical storage capacity [21]. The cross-sectioned images of the NiCo_2O_4 films in Fig. 2d, e showed the thickness of the prepared film, which varies from 20 to 23 μm . The surface topography obtained by AFM as shown in Fig. 3 demonstrated that the as-prepared NiCo_2O_4 film has a 20 μm in thickness fabricated on top of ITO substrates. The AFM images illustrated important statistical quantities such as roughness of about 126 nm and the surface area of 70 μm^2 . As the film's roughness increases, the surface area increases, which makes more electrolyte distribution through its pores and surface so it can hold more charge without increasing the lateral dimensions of the capacitors [22]. Both SEM and AFM exhibited almost similar results regarding the surface topology and micro-structure of NiCo_2O_4 thin film.

The X-ray fluorescence (XRF) analysis has been carried out to provide insights into the elemental compositions of the NiCo_2O_4 sample. As shown in Fig. 4, the fluorescence signals characteristic include K_α and K_β of cobalt and nickel sample. The Indium fluorescence signal appeared in tiny amounts and came from the ITO substrate. The inset table in Fig. 4 shows the mass percentage for the elemental component of the NiCo_2O_4 thin film. It is observed that 93.5% of the thin-film mass is for nickel and cobalt, which is an indication of the high purity of the thin film.

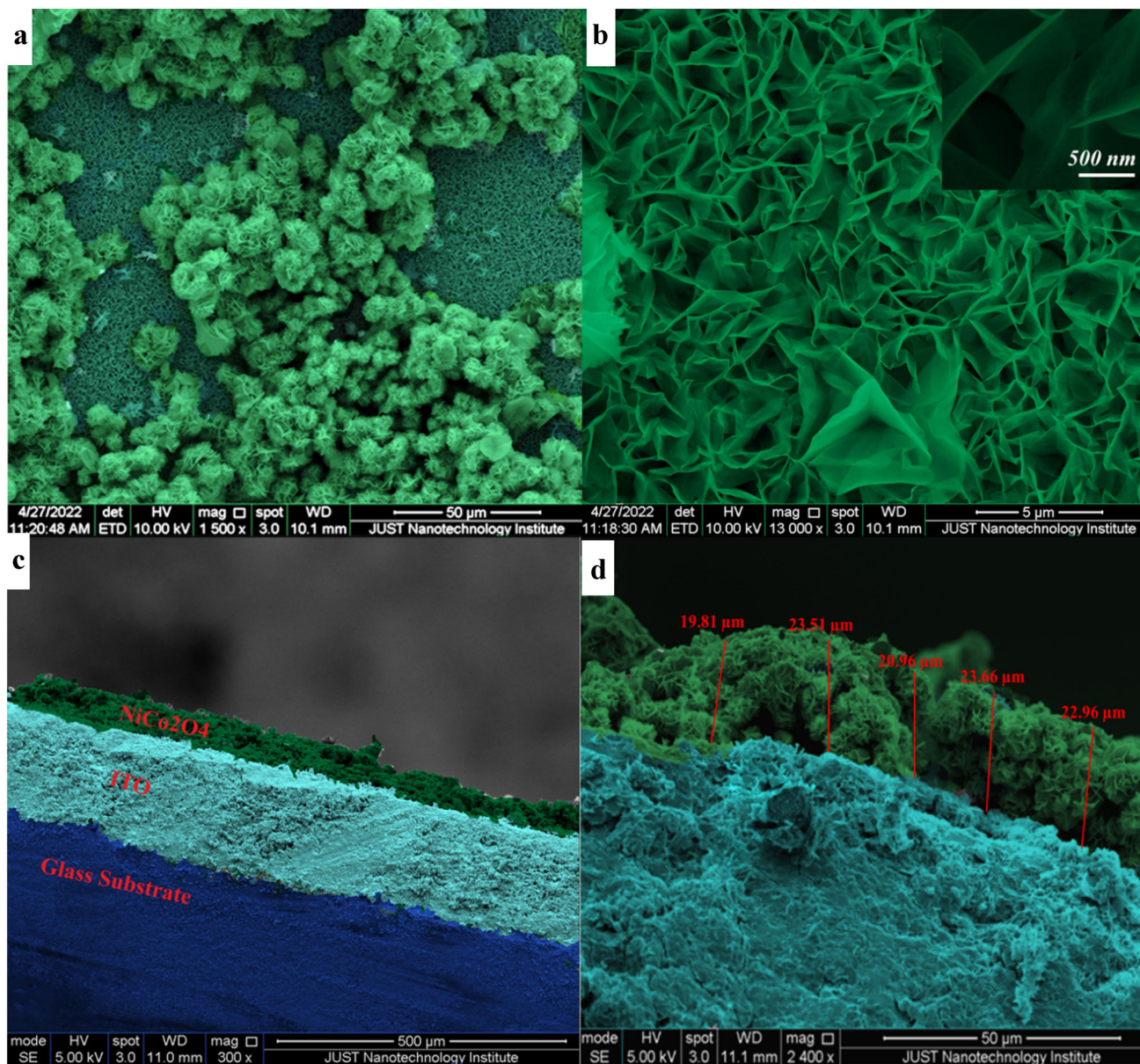


Fig. 2 Surface morphologies of NiCo_2O_4 films at scales of **a** 50 μm , **b** 5 μm , **b** 5 μm (inset: 500 nm), and cross section of as-prepared film at scales **c** 500 μm and **d** 50 μm

3.2 Electrochemical measurements

The electrochemical reaction of NiCo_2O_4 with the KOH electrolyte can be written as follows [23]:



where $\text{NiCo}_2\text{O}_4 \parallel \text{OH}^-$ represents the electric double layer formed by the hydroxyl ion, and $\text{NiCo}_2\text{O}_4\text{-OH}$ represents the product formed by the cathode reaction involving the hydroxyl ion.

The electrochemical measurements of the as-prepared nanosheet electrodes were characterized by cyclic voltammetry (CV) in a potential window between 0.1 and 0.8 V at scan rates of 10, 30, 50, and 100) mV/s as illustrated in Fig. 5, galvanostatic charge–discharge (GCD) in a potential window between 0 and 0.65 V, and the electrochemical impedance spectroscopy (EIS) techniques with a frequency range from 0.01 Hz to 100 kHz. Specific capacitance (C_s) can be evaluated based on charge–

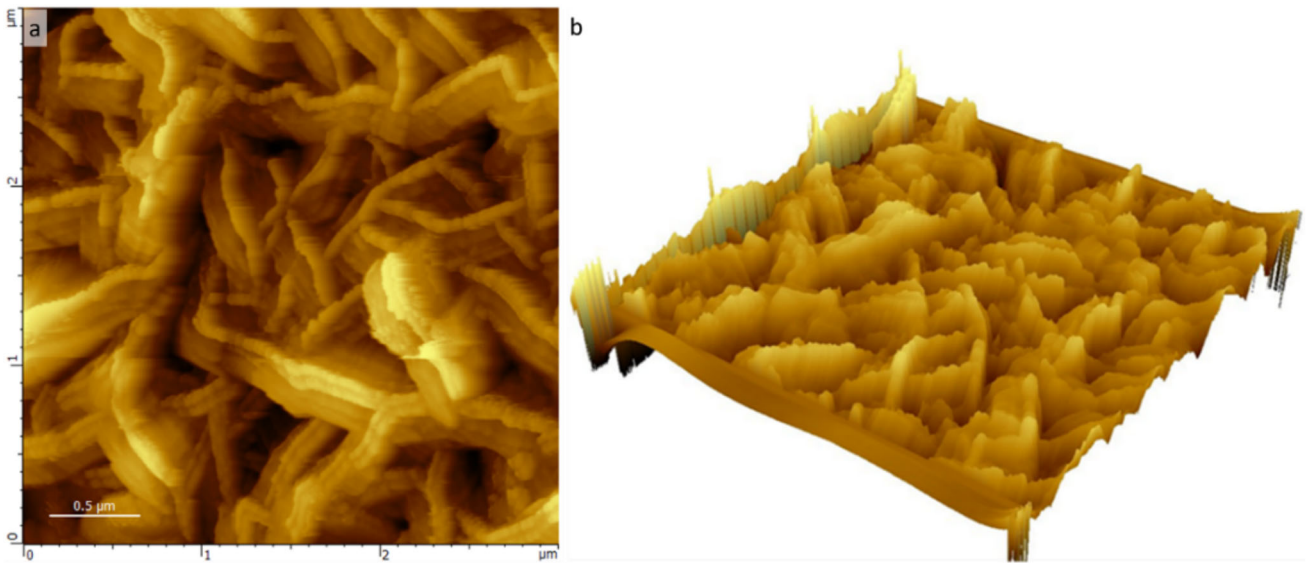


Fig. 3 AFM images for NiCo₂O₄ thin film in 2D view (left) and 3D mode (right)

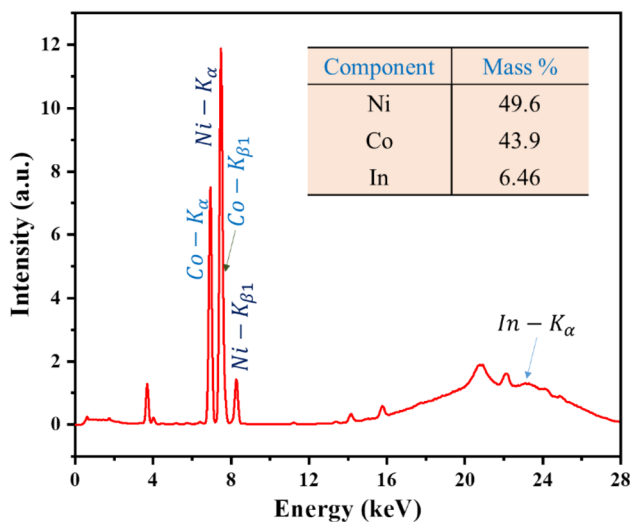


Fig. 4 X-ray fluorescence (XRF) spectra of the NiCo₂O₄ film sample

discharge curve according to the following formula [24]:

$$C_s = \frac{I\Delta t}{m\Delta V}, \tag{2}$$

where C_s represents the specific capacitance in (F/g), I (mA), Δt (sec), ΔV (Volt) and m (mg) are the charge-discharge current, the discharge time, the potential window of discharge process, and the mass of the active materials in the electrodes, respectively.

The CV curves for KOH and H₂SO₄ show a slight difference in an electrochemical redox reaction. Furthermore, showing a quasi-rectangular CV shape

which is in agreement with the typical pseudocapacitive behavior of supercapacitor [25]. However, the KOH and H₂SO₄ electrolytes exhibit almost similar integral areas.

EIS measurements were carried out towards further understanding the superior pseudocapacitive performance of the NiCo₂O₄ electrodes. Nyquist plots as shown in Fig. 6 show a semicircle arc at high-frequency scale and linear region at low frequency in KOH medium. Meanwhile, only, linear behavior is observed in H₂SO₄ medium. The EIS data for the electrodes were fitted with the NOVA (version 2.1.5) software. The equivalent circuit that is employed to fit the EIS spectra is presented in the inset in Fig. 6. The fitting parameters, R_s are the series resistance which is related to the resistance to ions of the electrolyte and the electron transport of the electrodes and current collectors, (R_p) is the charge-transfer resistance associated with the Faradic reactions at the electrode/electrolyte interface, W is the Warburg resistance use to it the linear region of EIS curve and arisen from the ion diffusion and transport in the electrolyte [26, 27].

The series resistance can be valued from the intercept at the real axis at the high-frequency region. The NiCo₂O₄ electrode exhibits an equivalent R_s value of 135Ω in KOH medium and 472 Ω in H₂SO₄ medium [26]. In addition, the charge-transfer resistance (R_p) in KOH medium is much less than resistance in H₂SO₄ medium. Meanwhile, the NiCo₂O₄ electrode in H₂SO₄ solution shows no obvious

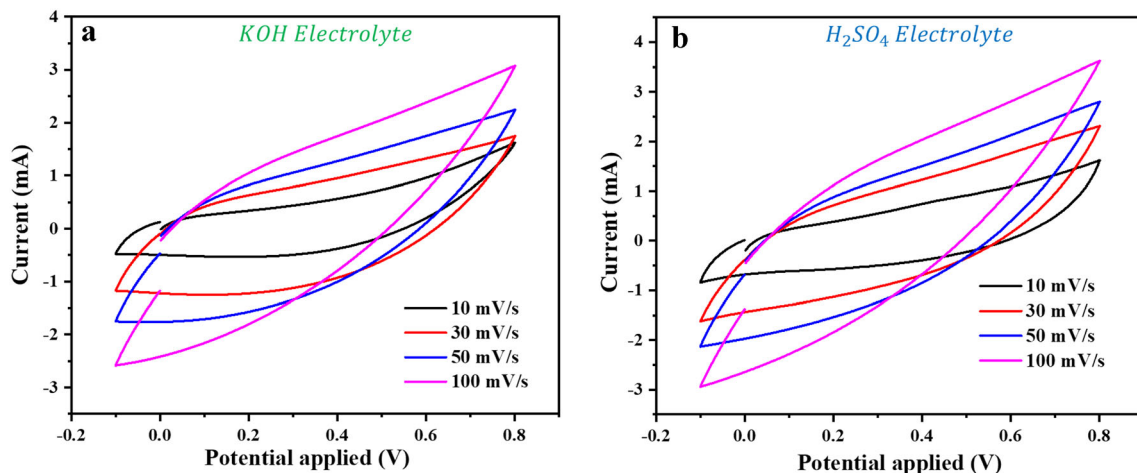


Fig. 5 Cyclic voltammograms of NiCo₂O₄ nanosheets for **a** 1 M KOH and **b** 1 M H₂SO₄ electrolyte solutions

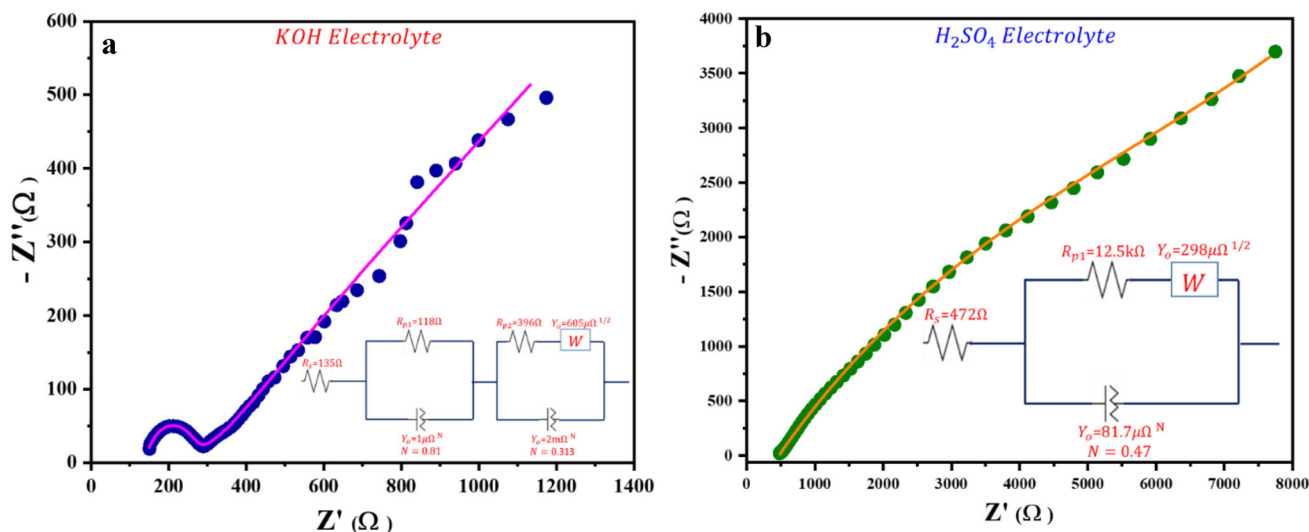


Fig. 6 Nyquist plots of NiCo₂O₄ asymmetric supercapacitor and equivalent circuit in **a** KOH medium and **b** H₂SO₄ electrolytes

semicircle in the high-frequency region, which indicates the fast charge transfer of H⁺ ions caused by the Faradic reaction and ionic diffusion is the only electrochemical reaction that could be observed in H₂SO₄ solution [27]. Therefore, highly conductive material to the current collector design is favorable for high-performance electrochemical application.

Bode plot provides insight into the capability rate of the electrodes. Figure 7a,b shows impedance and phase angle varying with frequency scale in KOH and H₂SO₄ electrolytes, respectively. The higher phase angle in KOH electrolyte at low and high frequency suggested good supercapacitive characteristics compared to H₂SO₄ solutions. The Bode plot for H₂SO₄ indicates a hump at an intermediate

frequency, which is the facilitate electrolyte ion diffusion and enhances supercapacitive performance. The Bode plot at low frequency (0.1 Hz) has a phase angle ϕ of 18° in KOH and ϕ of 23° in H₂SO₄ indicating a better capacitive retention in H₂SO₄ electrolyte [28]. This result is quite consistent with the nature of the electrolytes, which is an ionic solution (K⁺, OH⁻, H⁺, SO₄⁻), offering higher resistance to ion insertion and de-insertion.

Fig. 8 shows the GCD curves of NiCo₂O₄-based supercapacitor at different current densities ranging from 0.06 to 0.1 mA within the potential window ranging of 0 to 0.65 V. The plateaus observed clearly in the discharge curves revealed a typical pseudocapacitive behavior, indicating the as-prepared sample

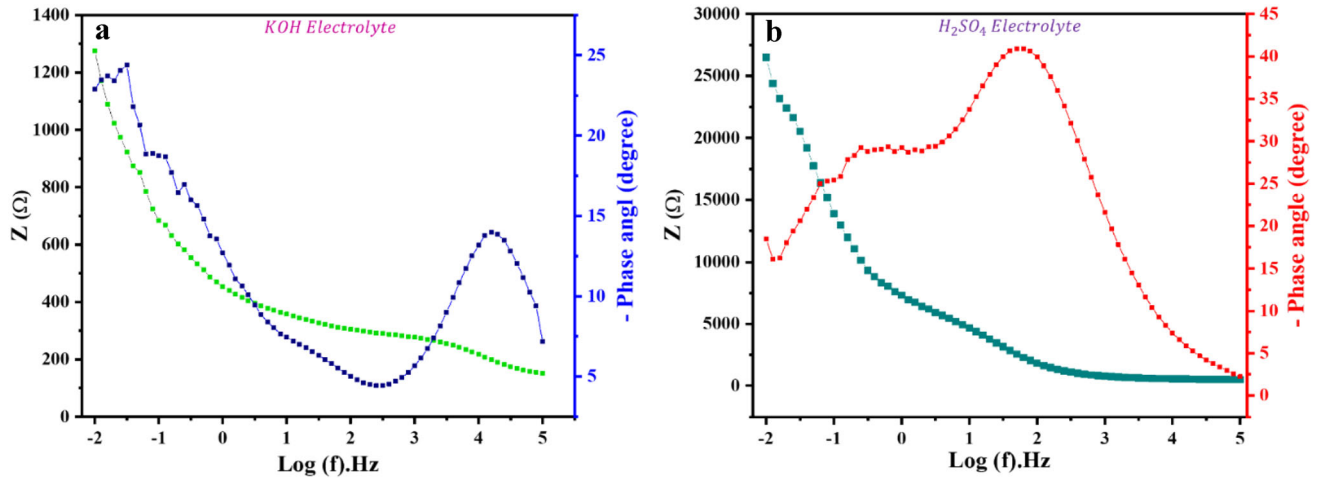


Fig. 7 Bode plots of NiCo₂O₄ asymmetric supercapacitor using **a** KOH and **b** H₂SO₄ electrolytes

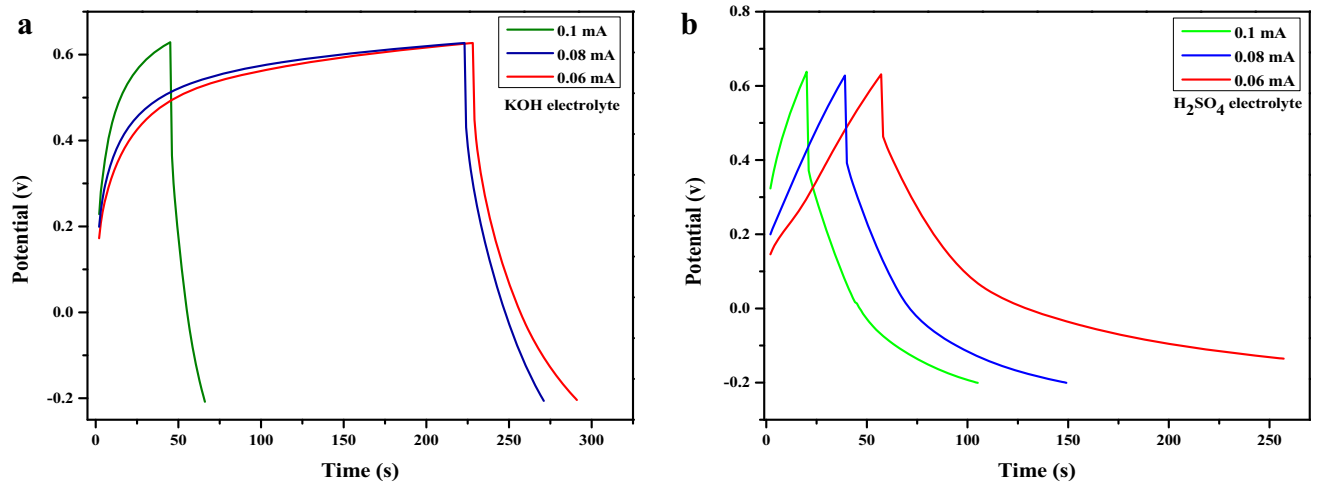


Fig. 8 Galvanostatic charge–discharge curves at different currents of NiCo₂O₄ asymmetric supercapacitor using **a** KOH and **b** H₂SO₄ electrolytes

as a typical pseudocapacitor electrode material [29]. According to Eq. (1), it can be calculated that the specific capacitance of

the as-prepared samples with KOH electrolyte is 235 F/g at current of 0.06 mA, while that of the as-prepared samples with H₂SO₄ electrolyte is 723 F/g. The calculated specific capacitances of the as-prepared samples at different current densities ranging from 0.06 to 0.1 mA are plotted in Fig. 9, and it can be seen that the as-prepared samples with H₂SO₄ electrolyte exhibit excellent specific capacitances of 723 F/g, 540 F/g, and 510 F/g compared to that in KOH electrolyte of 130 F/g, 215 F/g, and 235 F/g at current densities ranging from 0.06, 0.08, to 0.1 mA, respectively.

This result indicates that pseudocapacitive properties are in agreement with behavior of CV curves and EIS curves. Further, a conductive network through NiCo₂O₄ nanoflakes in hybrid electrodes offers a short electron and ion diffusion pathway and charge transfer at the interface [30, 31]. It is observed that the discharge time in H₂SO₄ electrolyte is greater than KOH electrolyte and varied with different current densities, which may be a result of the slower charge transfer into the inner region of pores of hybrid structures at higher potential applied. This result could be assigned to high-charge storage capacity at higher applied potential [32].

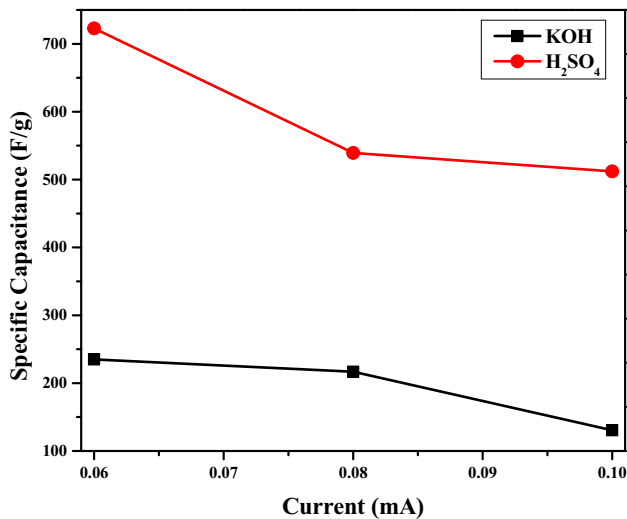


Fig. 9 The specific capacitance of the as-prepared electrode in KOH and H₂SO₄ electrolyte at various current densities

4 Conclusion

In summary, NiCo₂O₄ metal oxide was hydrothermally deposited over a cleaned ITO substrate. SEM and AFM images confirmed the presence of nanosheet structure of the as-prepared sample, which had an overall roughness of 126 nm. A hybrid supercapacitor made of an anode electrode of NiCo₂O₄ and a cathode of graphite separated by filter paper. At various voltage scan rates, cyclic voltammetry of a supercapacitor device in KOH and H₂SO₄ electrolyte revealed a quasi-rectangular shape. This behavior is attributed to the pseudocapacitive mechanism. Furthermore, the linear region and semicircle arc of the EIS curve confirm the fabricated device's pseudocapacitive characteristics. Equivalent circuit-fitting parameters R_p and W were related to the charge-transfer resistance and ionic diffusion at the interface. The calculated specific capacitance according to the charge–discharge curves at current density of 0.06 mA found to be 130 F/g in KOH electrolyte and 723 F/g in H₂SO₄ electrolyte. Based on our results, the as-prepared NiCo₂O₄ nanosheets' thin films can be used as a good candidate for supercapacitor and energy storage application using a simple and cost-effective hydrothermal process.

Acknowledgements

The authors acknowledge the financial support provided by Jordan University of Science and Technology (JUST) through Grant No.197/2022.

Author contribution

All authors contributed to the study conception and design. Material preparation, data collection, and analysis were performed by SA, BA, BA, AA, AA-O, and HM. The first draft of the manuscript was written by BA, SA, and all authors commented on previous versions of the manuscript. All authors read and approved the final manuscript. All data generated or analyzed during this study are included in this manuscript.

Funding

The financial support was provided by Jordan University of Science and Technology (JUST) through the Grant No.197/2022.

Data availability

Research data policy and data availability statements were considered during the manuscript submission process.

Declarations

Conflict of interest Competing interests between authors do not exist during the preparation of this manuscript. The authors declare that no funds, grants, or other support were received during the preparation of this manuscript. The authors have no relevant financial or non-financial interests to disclose.

References

1. B. Pollet et al., Fuel-cell (hydrogen) electric hybrid vehicles, in *Alternative fuels and advanced vehicle technologies for improved environmental performance*. (Elsevier, Amsterdam, 2014), pp.685–735

2. R. Packiaraj et al., Unveiling the structural, charge density distribution and supercapacitor performance of NiCo₂O₄ nano flowers for asymmetric device fabrication. *J. Energy Storage* **34**, 102029 (2021)
3. F. Wu et al., O and N co-doped porous carbon derived from crop waste for a high-stability all-solid-state symmetric supercapacitor. *New J. Chem.* **46**(41), 19667–19674 (2022)
4. X. Wang et al., Achieving high rate performance in layered hydroxide supercapacitor electrodes. *Adv. Energy Mater.* **4**(6), 1301240 (2014)
5. S.W. Donne, M.F. Dupont, Separating the faradaic and non-faradaic charge storage mechanisms in electrochemical capacitors using step potential electrochemical spectroscopy. *ECS Meet. Abstr.* (2015). <https://doi.org/10.1149/MA2015-02/9/572>
6. B. Cui et al., Photophysical and photocatalytic properties of core-ring structured NiCo₂O₄ nanoplatelets. *J. Phys. Chem. C* **113**(32), 14083–14087 (2009)
7. N.A. Algadri, A.M. AL-Diabat, N.M. Ahmed, Zinc sulfide based thin film photodetector prepared by spray pyrolysis. *Instrum. Sci. Technol.* (2022). <https://doi.org/10.1080/10739149.2022.2108832>
8. M. Yu, X. Feng, Thin-film electrode-based supercapacitors. *Joule* **3**(2), 338–360 (2019)
9. V.C. Lokhande et al., Supercapacitive composite metal oxide electrodes formed with carbon, metal oxides and conducting polymers. *J. Alloys Compd.* **682**, 381–403 (2016)
10. J. Liu et al., Three-dimensional tubular arrays of MnO₂–NiO nanoflakes with high areal pseudocapacitance. *J. Mater. Chem.* **22**(6), 2419–2426 (2012)
11. W. Raza et al., Recent advancements in supercapacitor technology. *Nano Energy* **52**, 441–473 (2018)
12. A. Jagadale et al., Performance evaluation of symmetric supercapacitor based on cobalt hydroxide [Co(OH)₂] thin film electrodes. *Electrochim. Acta* **98**, 32–38 (2013)
13. S. Kandalkar et al., Chemical synthesis of cobalt oxide thin film electrode for supercapacitor application. *Synth. Met.* **160**(11–12), 1299–1302 (2010)
14. Y.-Z. Zheng, H.-Y. Ding, M.-L. Zhang, Preparation and electrochemical properties of nickel oxide as a supercapacitor electrode material. *Mater. Res. Bull.* **44**(2), 403–407 (2009)
15. G. Han et al., Short-range diffusion enables general synthesis of medium-entropy alloy aerogels. *Adv. Mater.* **34**(30), 2202943 (2022)
16. S. Giri, D. Ghosh, C.K. Das, One pot synthesis of ilmenite-type NiMnO₃–“nitrogen-doped” graphene nanocomposite as next generation supercapacitors. *Dalton Trans.* **42**(40), 14361–14364 (2013)
17. G. Zhang, Controlled growth of NiCo₂O₄ nanorods and ultrathin nanosheets on carbon nanofibers for high-performance supercapacitors. *Sci. Rep.* **3**(1), 1–6 (2013)
18. X. Guo et al., Engineering electron redistribution of bimetallic phosphates with CeO₂ enables high-performance overall water splitting. *Chem. Eng. J.* **453**, 139796 (2023)
19. L. Zhou et al., Metal oxides in supercapacitors, in *Metal oxides in energy technologies*. (Elsevier, Amsterdam, 2018), pp.169–203
20. F. Béguin et al., Carbons and electrolytes for advanced supercapacitors. *Adv. Mater.* **26**(14), 2219–2251 (2014)
21. M. Yang et al., Self-assembly of three-dimensional zinc-doped NiCo₂O₄ as efficient electrocatalysts for oxygen evolution reaction. *Chemistry: Eur. J.* **24**(49), 13002–13008 (2018)
22. I.T. Papadas et al., Low-temperature combustion synthesis of a spinel NiCo₂O₄ hole transport layer for perovskite photovoltaics. *Adv. Sci.* **5**(5), 1701029 (2018)
23. D. Choi, G.E. Blomgren, P.N. Kumta, Fast and reversible surface redox reaction in nanocrystalline vanadium nitride supercapacitors. *Adv. Mater.* **18**(9), 1178–1182 (2006)
24. Q. Liu et al., Manganese dioxide core–shell nanostructure to achieve excellent cycling stability for asymmetric supercapacitor applications. *RSC Adv.* **7**(53), 33635–33641 (2017)
25. P.S. Shewale, K.-S. Yun, NiCo₂O₄/RGO hybrid nanostructures on surface-modified Ni core for flexible wire-shaped supercapacitor. *Nanomaterials* **11**(4), 852 (2021)
26. Y. Zhang, Z. Guo, Honeycomb-like NiCo₂O₄ films assembled from interconnected porous nanoflakes for supercapacitor. *Mater. Chem. Phys.* **171**, 208–215 (2016)
27. S. Khalid et al., Microwave assisted synthesis of porous NiCo₂O₄ microspheres: application as high performance asymmetric and symmetric supercapacitors with large areal capacitance. *Sci. Rep.* **6**(1), 1–13 (2016)
28. H.K. Hassan et al., Ruthenium nanoparticles-modified reduced graphene prepared by a green method for high-performance supercapacitor application in neutral electrolyte. *RSC Adv.* **7**(19), 11286–11296 (2017)
29. Z. Wang et al., Co(OH)₂@FeCo₂O₄ as electrode material for high performance faradaic supercapacitor application. *Electrochim. Acta* **299**, 312–319 (2019)
30. L.L. Zhang et al., Highly conductive and porous activated reduced graphene oxide films for high-power supercapacitors. *Nano Lett.* **12**(4), 1806–1812 (2012)
31. L. Zhang, G. Shi, Preparation of highly conductive graphene hydrogels for fabricating supercapacitors with high rate capability. *J. Phys. Chem. C* **115**(34), 17206–17212 (2011)

32. D. Gandla, H. Chen, D.Q. Tan, Mesoporous structure favorable for high voltage and high energy supercapacitor based on green tea waste-derived activated carbon. *Mater. Res. Express* 7(8), 085606 (2020)

Publisher's Note Springer Nature remains neutral with regard to jurisdictional claims in published maps and institutional affiliations.

Springer Nature or its licensor (e.g. a society or other partner) holds exclusive rights to this article under a publishing agreement with the author(s) or other rightsholder(s); author self-archiving of the accepted manuscript version of this article is solely governed by the terms of such publishing agreement and applicable law.